UNLIMITED

RSRE
MEMORANDUM No. 4348

ROYAL SIGNALS & RADAR ESTABLISHMENT

THEORETICAL AND EXPERIMENTAL COMPARISON OF INFRA-RED AND VISIBLE LASER SCATTERING FROM A VARIETY OF SURFACE TYPES

Authors: D L Jordan, R C Hollins, E Jakeman & A Prewett

PROCUREMENT EXECUTIVE,
MINISTRY OF DEFENCE,
R S R E MALVERN,
WORCS.

RSRE MEMORANDUM No. 4348

ROYAL SIGNALS AND RADAR ESTABLISHMENT

Memorandum 4348

Title: THEORETICAL AND EXPERIMENTAL COMPARISON OF INFRA-RED AND VISIBLE LASER SCATTERING FROM A VARIETY OF SURFACE TYPES

Authors: D L Jordan, R C Hollins, E Jakeman and A Prewett

Date: March 1990

SUMMARY

A comparison is made between theorectical predictions of the angular distribution of laser radiation scattered from a variety of rough surfaces and experimental measurements of fractal one. The surfaces were initially well characterised using a mechanical stylus instrument to determine the surface profiles. Scattering experiments were then carried out using both transmissive and reflective geometries and both visible and infra-red radiation. The results show that fractal models are appropriate in the infra-red region, whereas single scale models give better agreement with experimental results in the visible region.

RSRE MEMORANDUM NO 4348

THEORETICAL AND EXPERIMENTAL COMPARISON OF INFRA-RED AND VISIBLE LASER SCATTERING FROM A VARIETY OF SURFACE TYPES

D L Jordan, R C Hollins, E Jakeman and A Prewett

CONTENTS

1 INTRODUCTION

2 THEORY

3 EXPERIMENT

4 RESULTS AND DISCUSSION

5 SUMMARY AND CONCLUSIONS

6 REFERENCES

1 INTRODUCTION

The measurement of surface roughness is extremely important in many areas of optics, engineering and solid-state materials growth. The internationally adopted industrial measuring standard relies primarily on the measurement of surface profiles with a stylus instrument[1]. In this system the surface to be measured is probed by a diamond stylus whose vertical motions are registered. Unfortunately this suffers from a number of serious disadvantages such as the linear probing and time-consuming measuring process which renders it unsuitable for 'on-line' production systems, its tendency to damage delicate surfaces and its inability to reliably measure roughnesses less than ~ 0.01 μm. When however light is scattered from a rough surface the parameters of the statistical variations of scattered light depend on those of the surface roughness. Consequently much effort[1,2,3] has been devoted over the past few years, with varying degrees of success, to utilising the scattering of optical radiation from a surface as a means of determining its characteristics.

The basic features of scattering by rough surfaces can be treated by two physical optics approaches. One is the rough surface treatment of Beckmann[4] which is directly applicable to reflective geometries; the other, which is generally applied to transmissive systems is based on the concept of a phase-changing screen. This simply introduces random phase variations into an initially plane monochromatic wave. Amplitude fluctuations then develop during the course of free propagation beyond the scattering plane. Transformations to either system can in principle be made to allow both transmissive and reflective geometries to be handled by either approach[5].

In general, the inverse scattering problem cannot be uniquely solved. Consequently it is necessary to develop a mathematical model of scattering and then test it experimentally. Most such treatments, both of the rough reflective surface and the phase-screen problem have assumed that the surface height fluctuations constitute a joint-Gaussian process so that only the correlation function or spectrum of the fluctuations is needed to complete the statistical model. Most workers have also, for mathematical convenience, adopted a Gaussian model for the spectrum; this corresponds physically to a smoothly varying surface containing fluctuations of roughly the same characteristic size. When both this length and the surface height variations are comparable to, or exceed the wavelength of the incident radiation this type of surface leads to amplitude fluctuations which are dominated by geometrical optics effects - caustics or singularities in the scattered ray density pattern[6,7]. Unfortunately experiments with rigid diffusers often show a different scattering behaviour[8,9] which is not consistent with the predictions of smoothly varying models.

One of the reasons for this is that solid scatterers are generally rough on many scales[10]. Hence predictions based on smooth single-scale surfaces are gross over-simplifications. Following Mandelbrot[11] the class of hierarchial or multi-scale surfaces possessing a simple power law spectrum have become known as fractals. Unlike smoothly varying surfaces, which are mathematically speaking 'continuous and differentiable to all orders', fractal surfaces are 'continuous but not differentiable' and contain random structure down to arbitrarily small scales. Consequently the concept of rays is inappropriate; only diffraction and interference effects occur[12].

There is a mounting body of evidence[10,13,14] to support the view that fractals may be a realistic model for many solid surfaces. However very little work[15,16] has been carried out to verify the predictions of fractal models on optical scattering. A particular area of interest and uncertainty for such models is the role played by scale sizes which are small compared to the wavelength of the incident radiation; these may not be properly included in the usual physical optics approximate formulation of the scattering problem.

In this Memorandum we present results of the mean scattered intensity as a function of scattering angle ($\langle I(\theta) \rangle$) from several targets, some of which are transmissive and some purely reflective. To ensure that the surfaces are well characterised over a large range of

scale sizes from well below to well above the probing wavelength, measurements have been carried out using a CO_2 laser of wavelength 10.6 μm. Also, because of the widespread use of He-Ne lasers in scattering experiments, the same scattering experiments have also been performed using such a laser, although its wavelength of 0.63 μm is comparable or less than the horizontal resolution limit of mechanical surface profile measuring instruments, and hence knowledge of scale sizes much below its wavelength is severely limited. Comparisons are then made with predictions of $\langle I(\theta) \rangle$ based on both fractal and smooth single-scale surface models.

The results shown in this Memorandum are an extension of some preliminary work presented in Reference 17; the aim here is to collate all such measurements obtained in a series of experiments.

2 THEORY

In this section we briefly outline the theories appropriate to the two extreme types of model mentioned, namely the single scale model and the fractal one. Some details of the equivalence between them is given in reference 5. For a perfectly conducting surface the field in the Fraunhofer region is given according to reference 4 by

$$E = E_o k F(\theta) \int_{-\infty}^{\infty} A(\underline{r}') \, e^{-i \, \underline{k}.\underline{r}'} \, G(\theta) \, e^{i \, k \, h(\underline{r}') f(\theta)} d^2\underline{r}' \qquad (1)$$

where E_o is the incident plane wave field, k is the wavevector of the incident radiation ($= 2\pi/\lambda$), $A(\underline{r}')$ defines the variation of intensity within the illuminated region and h(r') is the local surface height at position $\underline{r}'$. F, G and f are angle dependent terms given by

$$F(\theta) = \frac{1 + \cos\theta_1 \cos\theta_2 - \sin\theta_1 \sin\theta_2 \cos\theta_3}{\cos\theta_1 + \cos\theta_2} \qquad (2)$$

$$G(\theta) = \left[(\sin\theta_1 - \sin\theta_2 \cos\theta_3)^2 + \sin^2\theta_2 \sin^2\theta_3 \right]^{\frac{1}{2}} \qquad (3)$$

$$f(\theta) = \cos\theta_1 + \cos\theta_2 \qquad (4)$$

where θ_1, θ_2 and θ_3 are as defined in Fig 1. For normal incidence these simplify to

$$f(\theta) = 1 \qquad (5)$$

$$G(\theta) = \sin\theta_2 \qquad (6)$$

$$f(\theta) = 1 + \cos\theta_2 \qquad (7)$$

For the more normal phase-screen situation where the incident radiation is forward scattered i.e a transmission geometry, (1) is replaced, for normal illumination by[18]

$$E = E_o k (1 + \cos\theta) \int_{-\infty}^{\infty} A(\underline{r}') e^{-i \, k \, \underline{r}'.\underline{r}/R + i \, f(\theta) \varphi(\underline{r}')} d^2\underline{r}' \qquad (8)$$

where $\underline{r}/R = \sin\theta$ and $f(\theta)\varphi(\underline{r}')$ is the phase fluctuation introduced by the phase-screen at $\underline{r}'$. $f(\theta)$ is given by

$$f(\theta) = h\left[1 - \frac{\sin^2\theta_1}{n^2}\right]\left\{n - \left[1 - \frac{\sin^2\theta_1}{n^2}\right]^{\frac{1}{2}}\left[1 - \frac{\sin^2\theta_2}{n^2}\right]^{\frac{1}{2}} - \frac{\sin\theta_1}{n}\,\frac{\sin\theta_2}{n}\right\} \qquad (9)$$

where h is the local surface height above the mean plane.

For relatively small angles of incidence ($\lesssim 20^\circ$) and the high refractive index materials used in this work (> 2.4) this expression does not differ significantly from $(n - 1)$ for all scattering angles θ. For non-normal illumination the factor $(1 + \cos\theta)$ preceeding the integral in (8) is replaced by $(\cos\theta_1 + \cos\theta_2)$ and the phase term must be modified to include the mean slope of the phase screen with respect to the input beam.

It should be noted that (1) and (8) are limited to situations where the Kirchoff approximation is valid i.e to situations in which small-angle scalar diffraction theory is valid. As mentioned in the introduction this may be questionable for fractals because they include scale sizes less than the wavelength of the incident radiation. In practice, there will often be an inner scale or high frequency cut-off in the phase fluctuation spectrum of the scatterer. Provided the scattering power of inner scale sizes is small, by which is meant their rms 'height' is much smaller than a wavelength, then the basic scattering characteristics of the fractal model will be unaffected in near specular directions. However, small scale roughness will contribute to large angle scattering and so some doubt must exist as to the validity of Fraunhofer large angle scattering results obtained using a fractal model for $h(\underline{r}')$ in (1) and (8). This point will be considered further in the results and discussion section.

There are also a number of other, possibly serious approximations implicit in using (1) and (8) at large scattering angles. These include neglect of variations of transmissivity or reflectivity with angle, polarisation effects and shadowing. An approximate shadowing correction has however been used and will be outlined later. Nevertheless, in spite of these omissions, there is an accumulating body of experimental data which exhibits trends consistent with the predictions of equations (1) and (8) even at relatively large angles in the case of multi-scale surfaces.

For a smooth single scale surface, we adopt the normalised spatial autocorrelation function

$$\rho(\underline{r} - \underline{r}') = \frac{\langle h(\underline{r})h(\underline{r}')\rangle}{h_o^2} = \exp - \left[\frac{|\underline{r} - \underline{r}'|^2}{\xi^2}\right] \qquad (10)$$

where h_o^2 is the mean square surface height fluctuation and ξ the characteristic length scale. If h is a Gaussian process, the resulting mean scattered intensity which is equal to EE^*, is obtained from (1) as [16]

$$\langle I(\theta)\rangle = E_o^2 k^2 F^2(\theta) \int_{-\infty}^{\infty} \exp\left[-\frac{\underline{r}^2 + \underline{r}'^2}{w^2}\right]\left[\exp i\, \underline{k}.(\underline{r} - \underline{r}')G(\theta)\right]$$

$$\exp\left[-k^2 f^2(\theta)\left[1 - \rho(\underline{r} - \underline{r}')\right] h_o^2\right] d\,\underline{r}\, d\,\underline{r}' \qquad (11)$$

assuming the width of the gaussian profiled input beam is w.

The integral can be evaluated by the method of steepest descents when $k^2 f^2 h^2_o >> 1$ to give

$$\langle I(\theta)\rangle = \left[\frac{\pi^2}{2}\right] E_o^2 w^2 \left[\xi^2/h_o^2\right] \frac{F^2(\theta)}{f^2(\theta)} \exp\left\{-\frac{\xi^2}{4h_o^2}\frac{G^2(\theta)}{f^2(\theta)}\right\} \qquad (12)$$

In obtaining (12) from (11), the term $(1 - \rho(\underline{r} - \underline{r}'))$ has been expanded and only the first term retained. It also means that any even powered correlation function would give the same form as (12).

Assuming normal incidence and a reflective geometry, and neglecting inessential factors this results in

$$\langle I(\theta)\rangle \alpha \frac{1}{(1 + \cos\theta)^2} \exp\left\{-\frac{\xi^2}{4h_o^2}\frac{\sin^2\theta}{(1 + \cos\theta)^2}\right\} \qquad (13)$$

The equivalent expression for a transmission geometry derived via (8) for a phase-screen is

$$\langle I(\theta)\rangle \alpha \exp\left\{-\frac{\xi^2}{4h_o^2}\frac{\sin^2\theta}{(n-1)^2}\right\} \qquad (14)$$

where n is the refractive index of the phase-screen material.

Power law models for h are generally defined through the structure function

$$S(\delta) = \langle h(r) - h(r + \delta)^2\rangle = L^{2-\nu}\,|\delta|^{\nu} \qquad (15)$$

where $o < \nu < 2$ for a simple fractal surface. Following Sayles and Thomas[10] and Berry[19] L is called the topothesey and ν is related to the Hausdorff-Besicovitch dimension D of a section profile of a surface by $\nu = 2(2 - D)$. The spatial power spectrum P(k) of such a surface profile varies inversely as $(\text{frequency})^{\nu+1}$. The two parameters L and ν completely define a fractal surface.

For an isotropic two-dimensional scatterer the mean scattered intensity as a function of angle can be obtained from (1) (ie in a reflective geometry) in the Fraunhofer limit, assuming joint-Gaussian height fluctuations, by using a fractal model for the structure function. This gives

$$\langle I(\theta)\rangle \alpha k^2 F^2(\theta) \int_{-\infty}^{\infty} \exp\left[i\, \underline{k}.\underline{r}\, G(\theta)\right] \exp\left\{-\frac{1}{2} k^2 L^{2-\nu} r^{\nu} f^2(\theta)\right\} dr \qquad (16)$$

where various inessential angle independent terms have again been omitted. It is unfortunately necessary to perform integration numerically for arbitrary values of ν. However, for the special case of a Brownian fractal where $\nu = 1$, the integral may be evaluated analytically to give

$$\langle I(\theta)\rangle \alpha \frac{\frac{1}{2} k \cdot L\, f^2(\theta) F^2(\theta)}{\left[\frac{1}{4} k^2 L^2 f^4(\theta) + G^2(\theta)\right]^{3/2}} \tag{17}$$

For normal incidence (and a reflective geometry) this reduces to

$$\langle I(\theta)\rangle \alpha \frac{(1 + \cos\theta)^2}{\left\{\frac{1}{4} k^2 L^2 (1 + \cos\theta)^4 + \sin^2\theta\right\}^{3/2}} \tag{18}$$

For a transmissive phase-screen system the equivalent result is[15]

$$\langle I(\theta)\rangle \alpha \frac{1}{\left\{\frac{1}{4} k^2 L^2 (n - 1)^4 + \sin^2\theta\right\}^{3/2}} \times (1 + \cos\theta)^2 \tag{19}$$

where $f(\theta)$ as given in (9) is approximated by $(n - 1)$.

The very different forms of the angular dependence of the mean scattered intensity predicted on the basis of the fractal model ((18) and (19)) and the smooth single scale one ((13) and (14)) are immediately obvious. It should also be noted that $\langle I(\theta)\rangle$ predicted on the basis of a single scale model is independent of the wavelength of the scattering radiation. It is perhaps also worth pointing out that neither expression (12) nor expression (17) peak exactly in the specular direction. This effect turns out to be negligible for the surfaces investigated in the experiments reported in this paper.

At large scattering angles shadowing by the surface becomes important. This can be allowed for using the approximate theory of Bass and Fuks[20] which predicts that

$$\langle I(\theta)\rangle = \langle I(\theta)\rangle_{\text{no shadowing}} \times R(\theta_1, \theta_2) \tag{20}$$

where θ_1 is the input angle and θ_2 the scattering angle. $R(\theta_1, \theta_2)$ is given by

$$R(\theta_1, \theta_2) = \left\{1 + \Lambda(\theta_1) + \Lambda(\theta_2)\right\}^{-1} \tag{21}$$

where

$$\Lambda(\theta_j) = \tan\theta_j \int_{\cot\theta_j}^{\infty} \left\{m_{x_j} - \cot\theta_j\right\} p\left[m_{x_j}\right] dx_j \tag{22}$$

and m_x is the surface height slope at x, $p(m_x)$ being the distribution of slopes. For a Gaussian distribution of slopes

The output from the detector was fed to a low-noise premaplifier, thence to an amplifier with adjustable high and low pass filters and on to a phase-sensitive detector. The output from this was fed into a digital voltmeter and from this into a computer. The computer also controlled the rotating table. Scans were generally carried out either for reflection or transmission geometries with θ ranging from zero to 90° at a rate of 0.6 degrees sec^{-1}; eleven readings per second were taken. Slower scans were also taken over selected portions of the angular range. Generally eight scans were taken, the scatterer being moved across the beam between each one. The angle of incidence (θ_1) was generally zero for transmission geometries and up to 20° for reflection ones.

In this memorandum results are presented for several different targets. These are shot blasted germanium and zinc selenide discs, a sample of GaAs grown by a Metal Organic chemical vapour deposition technique on a 111 face rather than the more usual 110 face, and a sheet of computer print-out paper. The germanium, zinc selenide and gallium arsenide are transmitting at the infra-red wavelength used and hence allow both infra-red transmission and reflection measurements to be performed; their refractive indices at 10.6 μm are 4, 2.4 and 3.3 respectively. The zinc selenide sample was also transmissive in the visible He-Ne laser region.

For each of the target samples used several 5 mm long one-dimensional scans were made across the surface using a 'Talysurf' stylus instrument. This instrument had a height resolution of approximately 0.01 μm but could only take readings at 3.5 μm spacings, which is below the wavelength of the infra-red radiation used but well above that of the visible radiation. From these the structure functions and hence the topothesey and ν(via (15)) were obtained.

4 RESULTS AND DISCUSSION

The measured structure functions are shown on a logarithmic plot in Fig 3. The plots all show an approximate linear form over a range of scale sizes from somewhat below to somewhat above δ = 10 μm. This indicates that for each target, $S(\delta)$ follows an approximate power law and exhibits the self-affine behaviour of a fractal surface over a fairly wide range of scale sizes centred on 10 μm. Consequently it might be expected that the equations describing the scattering of the radiation based on a fractal model should give reasonable agreement with the infra-red measurements. The saturation of the curves at large separations shows the presence of an outer scale beyond which the fractal properties are not displayed.

Although, as stated the curves are reasonably linear around δ = 10 μm, some curvature in them is however apparent; at low values of δ in particular the slope appears to increase (topothesy decreasing, ν increasing) with decreasing scale size. The limited horizontal resolution of the tallysurf unfortunately precludes measurements being made at smaller values of δ, but these results do suggest that the surfaces may act differently in the visible region. Possibly they may even be more appropriately modelled as a single scale surface rather than a fractal one. A plot from a smooth single-scale surface as drawn on Fig 3 would have a slope of two for separations small compared to the scale size.

Similar curves to those shown in Fig 3 have been observed for a wide range of other surfaces ranging from metal to brick. A similar behaviour has also been observed by Thomas and Thomas[21] for ground and spark-eroded metals; these workers have also extended the lower measurable range of $S(\delta)$ to values of δ less than 1 μm. The fractal index ν and topothesey L as determined from the structure function plots (taken around the δ = 10 μm region) are also shown in Fig 3, as is the rms surface roughness h_σ. For all the surfaces and both laser wavelengths, the scattering phase change both in transmission ($kh_0(n-1)$) and reflection ($2kh_0$) is greater than unity (for normal incidence) though the path differences are significantly less than a wavelength in the 10 μm region.

However no significant breakthrough in unscattered component was observed for any of the samples studied.

The mean scattered intensity as a function of angle normalised to the peak intensity in the specular direction ($<I<\theta)>/I<S>$) is shown for the germanium, zinc selenide and gallium arsenide targets in transmission in Fig 4. Superimposed on the measured ZnSe and Ge results are curves derived assuming a fractal model for scattering (19) and using the values of ν and L derived from the tallysurf measurements (Fig 3). The correction for shadowing given in (21) has been applied; this is only significant for angles greater than 80°. It can be seen that for the CO_2 laser measurements the agreement between the measured and predicted curves is quite good out to surprisingly large angles.

At λ = 0.633 μm it is necessary to reduce the value of the measured topothesey from that appropriate to the λ = 10.6 μm results in order to obtain reasonable agreement with the measured curve; in this case from L = 0.13 μm to 0.08 μm, ν remaining equal to unity. As stated in section 2 this is not too surprising bearing in mind the apparent tendency of the gradient of the structue function verses displacement curve to increase at small scale sizes. It is also seen that the λ = 0.633 μm data can also be fitted equally well by a single scale model (14) with h_0 as given in Fig 3 and ξ = 6 μm. The λ = 10.6 μm data could not be fitted by such a model.

As expected the GaAs target which possessed a very high value of ν ($\simeq$ 1.8) and a very low value of L($\simeq$ 5 x 10^{-5} μm), and is therefore an approximation to a smooth-scale surface in the infra-red region, can be best fitted by such a model. The value of h_0 used in (14) was obtained from Fig 3. The surface height normalised autocorrelation function $\rho(\delta) = <h(x)h(x+\delta)>/<h^2>$ measured for this surface is shown in Fig 5. As expected it can be fitted quite well at low separations by a Gaussian of the form assumed in (10); the calculated curve with ξ = 18 μm is shown superimposed on Fig 5. This value of ξ has been in (14) to produce the theoretical fit in Fig 4. The agreement between theory and experiment is very good.

From the transmission results shown in Fig 4 it therefore appears that, as expected, the infra-red ZnSe and Ge target scattering can be well fitted by a fractal model using the tallysurf measured values of ν and L. Also, as suggested earlier, visible wavelength scattering from these surfaces might possibly be realistically modelled using a single-scale model. The GaAs results shows that a surface which can be shown from mechanical stylus measurements to behave as an approximate single scale surface at the appropriate infra-red scales, does in fact behave at such a target, and gives confidence in the scattering technique as a means to distinguish extreme surface types.

The reflection measurements are shown in Figs 6 and 7. Fig 6 shows both the infra-red and visible measurements made using the ZnSe target. As in transmission the infra-red results are well fitted using a fractal model (18) and the measured values of ν(=1) and L(= 0.13 μm) for angles out to ~ 45°. Beyond this there is a noticeable deviation between the measured and calculated results. A similar effect is seen for the infra-red Ge results shown in Fig 7. The reason for this is not known but as discussed in Section 2 the basis of the physical optics assumptions becomes more questionable at large scattering angles; this point is discussed in more detail later. As seen in both Figs 6 and 7, the use of a single-scale model to preduct the scattering in the infra-red region for both Ge and ZnSe gives very poor correlation between the measured and the calculated curves, even at small angles. In each case h_0 was determined from Fig 3 and ξ was chosen to give the 'best' fit (for Ge ξ = 18 μm and for ZnSe ξ = 45 μm).

In the visible region (λ = 0.633 μm) this situation is changed. As with the transmission measurements the value of L has to be reduced from its value given in Fig 3 (to 0.035 μm or Ge and 0.04 μm for ZnSe) to give reasonable agreement between theory and experiment when a fractal model is used. Again, as with the transmission results, a single scale model (13) gives an equally good fit. Finally, excellent agreement between

the reflection results obtained using the He-Ne laser and those calculated on the basis of the single scale model (ξ = 16 μm) is found for the paper target (Fig 7).

In order to determine whether depolarisation of the incident radiation was significant a rotatable wire grid polariser was attached to the front of the CO_2 detector housing and experimental runs performed first with the polariser in the same direction as the polarised laser radiation and then orthogonal to it. The cross-polarisation results for the Ge target in transmission is shown in Fig 8. This shows, on a log-linear plot the ratio of the scatterer intensity measured with the polariser orthogonal to the laser beam polarisation, to that with it aligned with the laser polarisation. The curve rises from approximately zero at small angles (limited by the discrimination of the polariser - 300:1) to approximately 15% at large angles; the rate of increase with angle slows considerably above about 50°. None of the surfaces gave a cross-polarisation term greater than 20%. This is almost certainly an upper limit because of the very small cross-polarised terms and hence the poor signal to noise ratio obtained. Consequently although not entirely negligible, depolarisation is by no means a dominant factor at any angle in these experiments.

5 SUMMARY AND CONCLUSIONS

Experimental measurements of the distributions of intensity scatterd by a variety of surfaces in both diffusing and reflective geometries have shown reasonable quantitative agreement with the predictions of a conventional physical optics approach to the scattering problem out to quite large angles. At 10.6 μm several of the surfaces exhibited the scattering characteristics expected for a fractal object with the measured parameters. At 0.6 μm, however, the distribution of intensity for these samples was equally well predicted by fractal or single scale models provided the model parameters were chosen appropriately. One surface was clearly of the single scale type when viewed at either wavelength, as expected from the contact measurements of its profile.

These results tend to confirm earlier conjectures that extreme surface types can be distinguished by a simple remote measurement of the intensity distribution of the scattered waves. They also demonstrate how different wavelengths can be used to probe the different regimes of roughness which are typical of rigid rough surfaces. The very sensitivities that we have explored, however, mitigate against exploiting observations of this kind for the purpose of developing a robust technique for surface remote sensing. Evidently, solid surfaces cannot in practice be characterised by single specific mathematical models containing few parameters: their height spectra are complex and in general variations in reflectivity, polarisation, and multiple scattering effects will further complicate the relationship between the scattered radiation and the surface profile. Moreover, often scattering measurements can only be made in one or two directions so that the full distribution of intensity is inaccessible. In these circumstances the higher order statistical properties of the intensity pattern generated by the surface as it moves through or is scanned by the illuminated region appear to provide the most promising line of investigation. Variation of the contrast of the scattered intensity pattern with the frequency spread of the illuminating wavelength is a direct measure of the height variations of the surface for example, whilst its dependence on illuminated area provides a measure of the effective density of surface inhomogeneities. In many situations of interest these may well be adequate measures of the surface characteristics. In others they will be adequate when supplemented by a priori knowledge. These ideas are not new[14], but their potential importance is confirmed by the results we have reported here.

ACKNOWLEDGEMENTS

The authors would like to acknowledge the help of G Hall in carrying out the tallysurf measurements and Dr P Oliver for providing the GaAs sample.

FIGURE CAPTIONS

Fig 1 General geometry for scattering from a rough surface.

Fig 2 Experimental arrangement

Fig 3 Experimentally measured structure functions

Fig 4 Normalised angular distributions of mean scattered intensity measured in a transmission geometry.

Fig 5 Surface height normalised autocorrelation function of the Gallium Arsenide surface.

Fig 6 Normalised angular distribution of mean scattered intensity of Zinc selenide target measured in a reflection geometry.

Fig 7 Normalised angular distribution of mean scattered intensity of germanium and paper targets measured in a reflection geometry.

Fig 8 Angular distribution of ratio of cross-polarised to polarised components of CO_2 radiation scattered from the germanium target

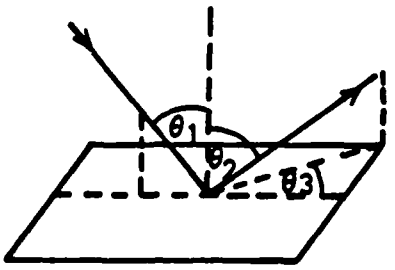

Figure 1 General geometry for scattering fron a rough surface

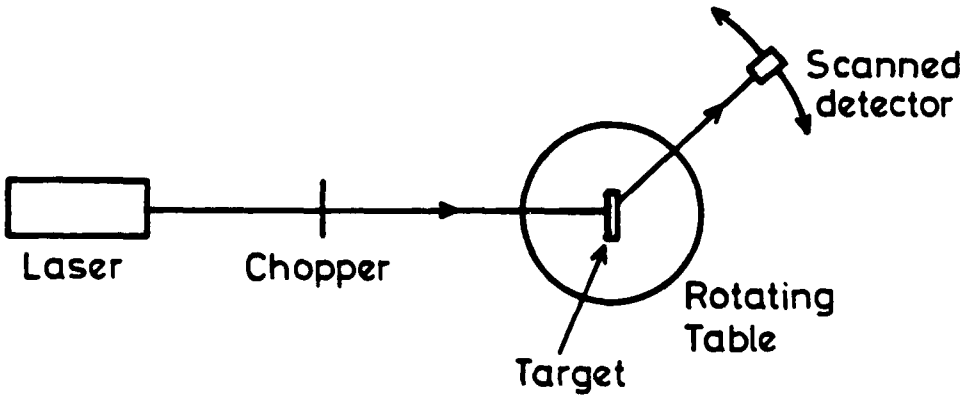

Figure 2 Experimental arrangement

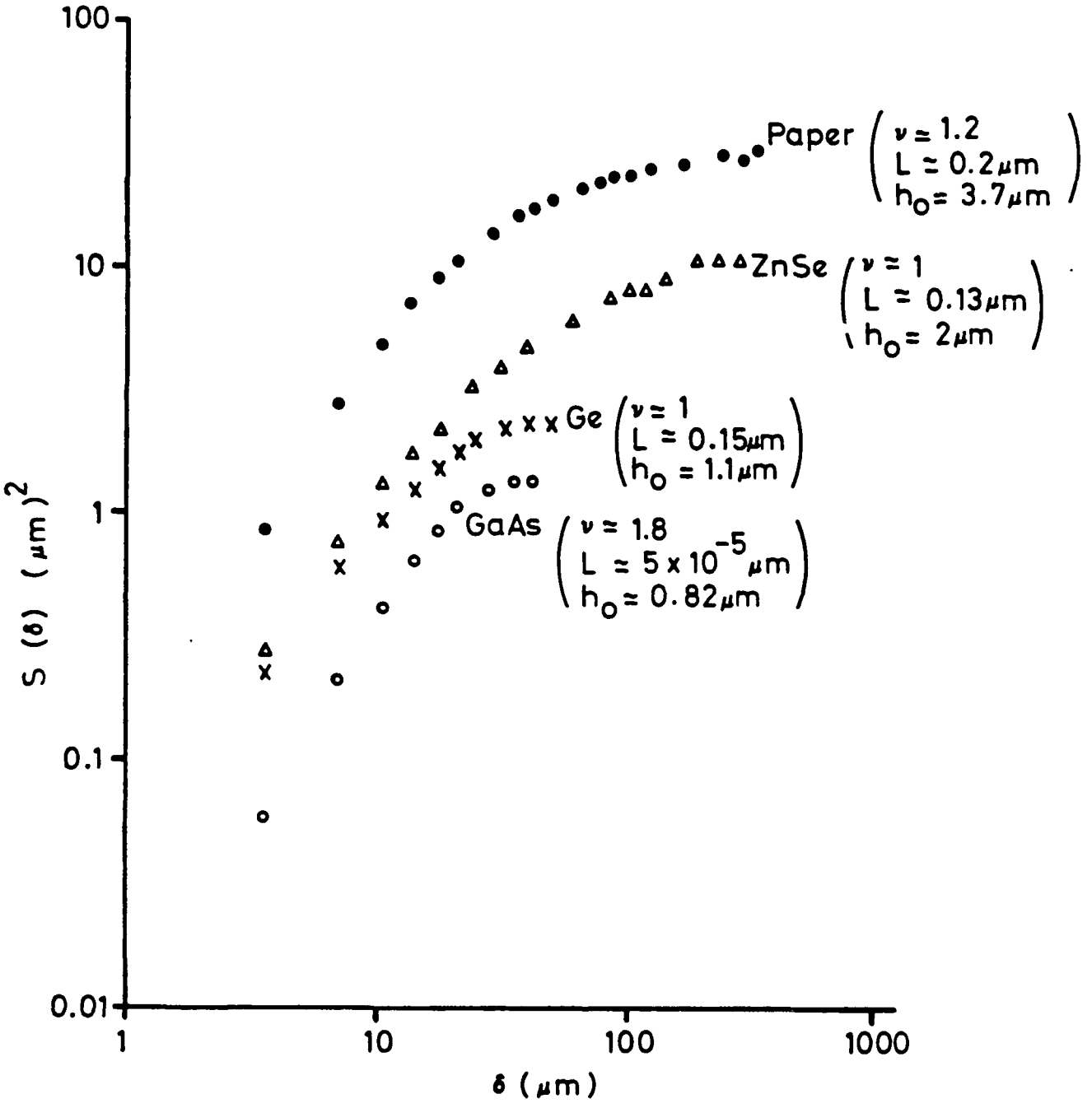

Figure 3 Experimentally measured structure functions

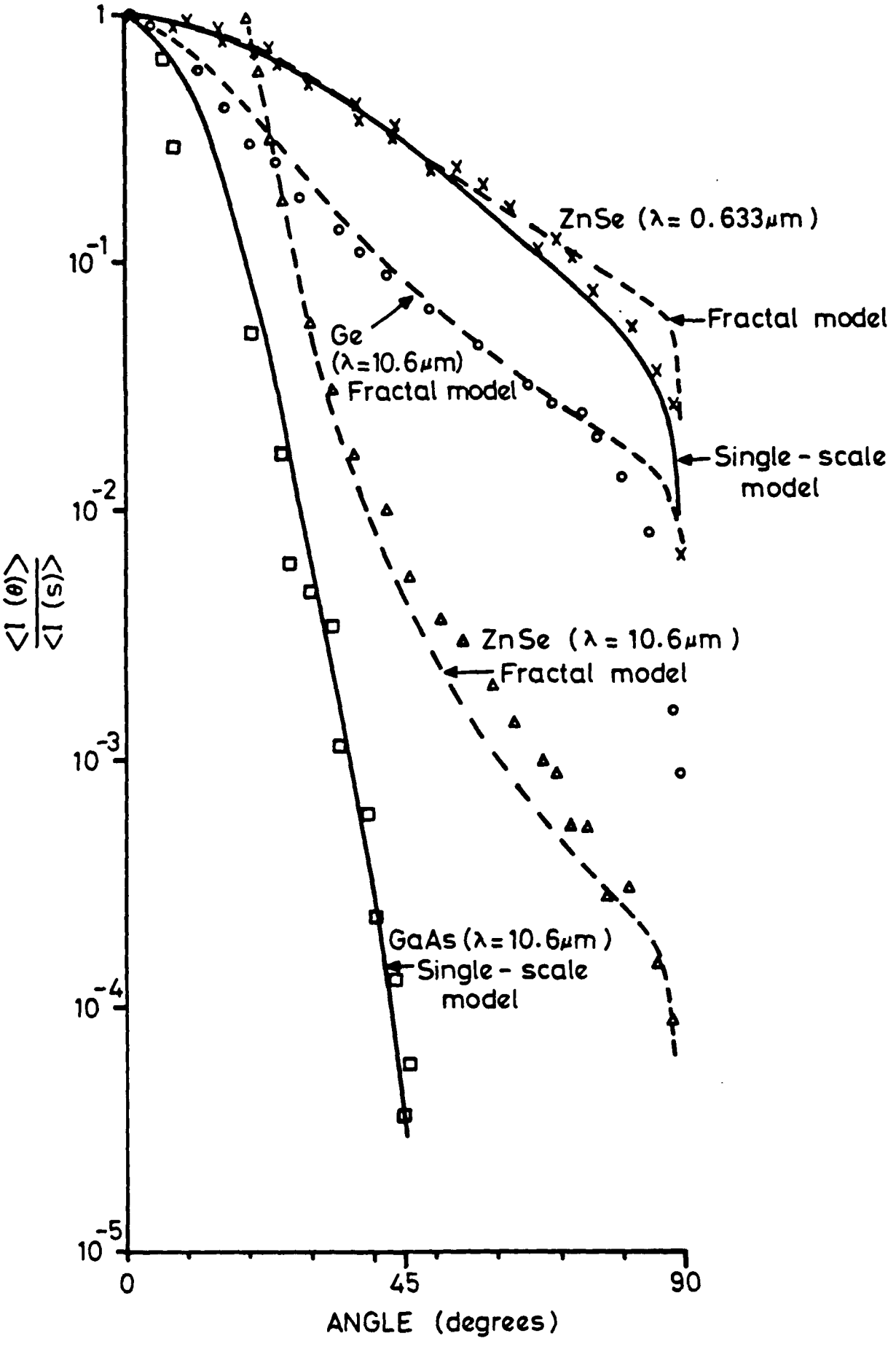

Figure 4 Normalised angular distributions of mean scattered intensity measured in a transmission geometry

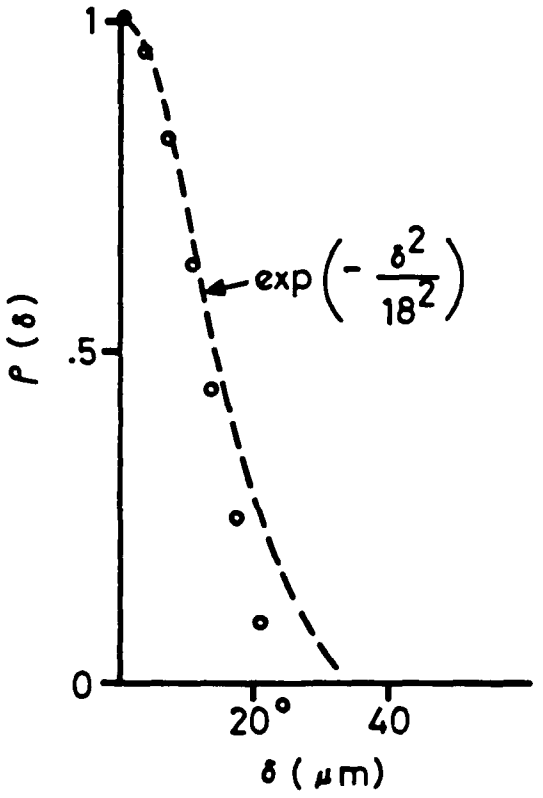

Figure 5 Surface height normalised autocorrelation function of the Gallium Arsenide surface

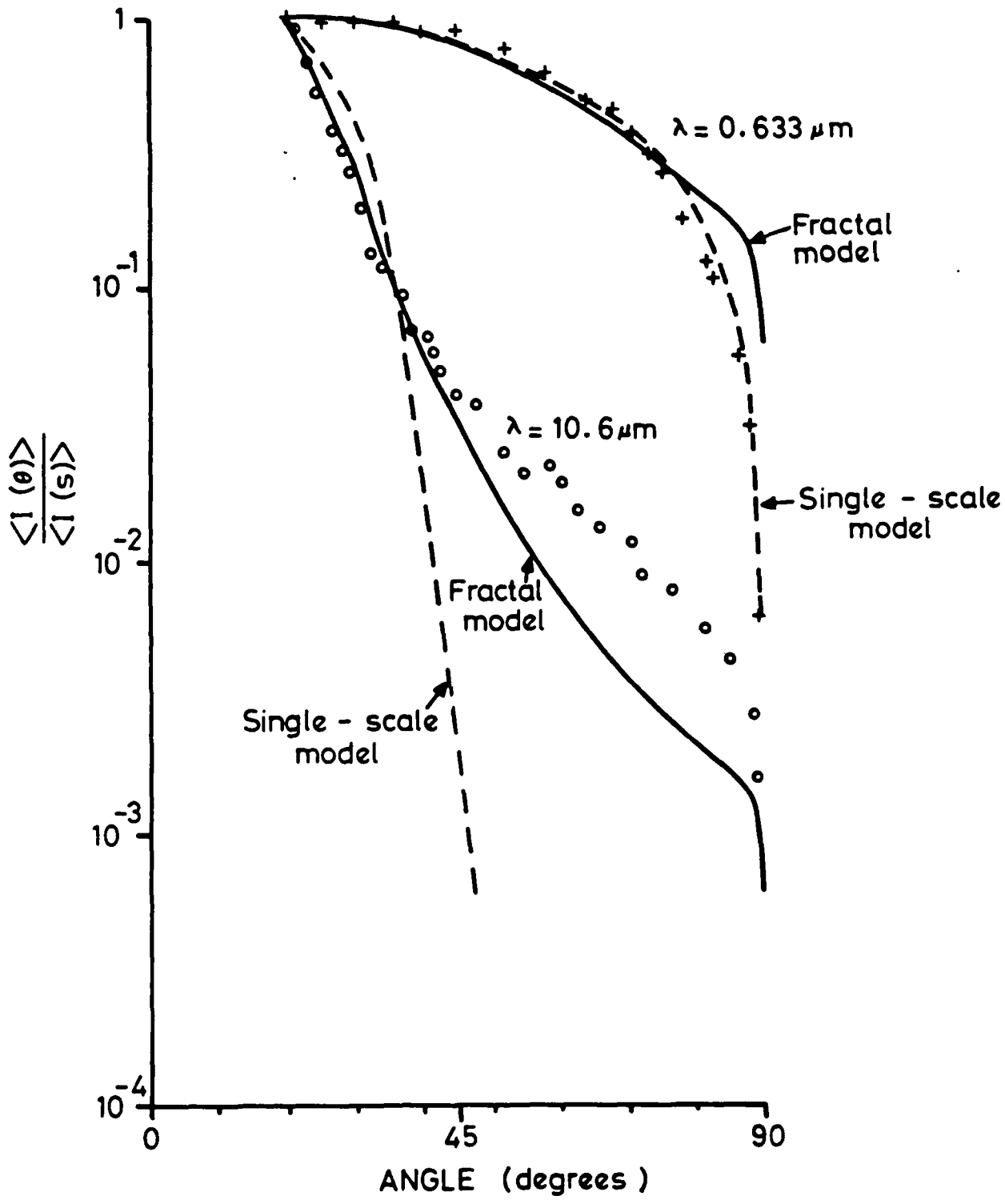

Figure 6 Normalised angular distribution of mean scattered intensity of Zinc selenide target measured in a reflection geometry

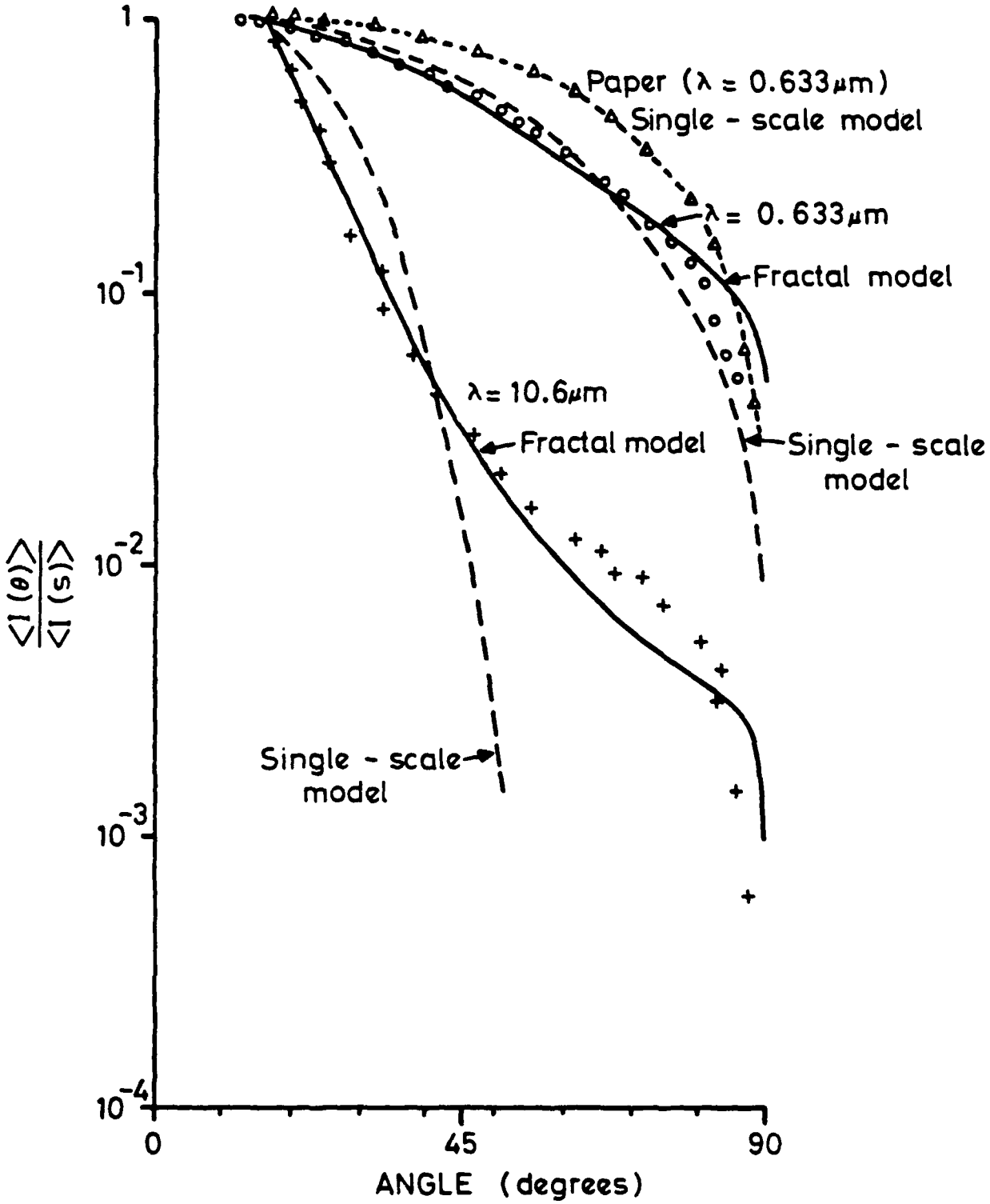

Figure 7 Normalised angular distribution of mean scattered intensity of germanium and paper targets measured in a reflection geometry

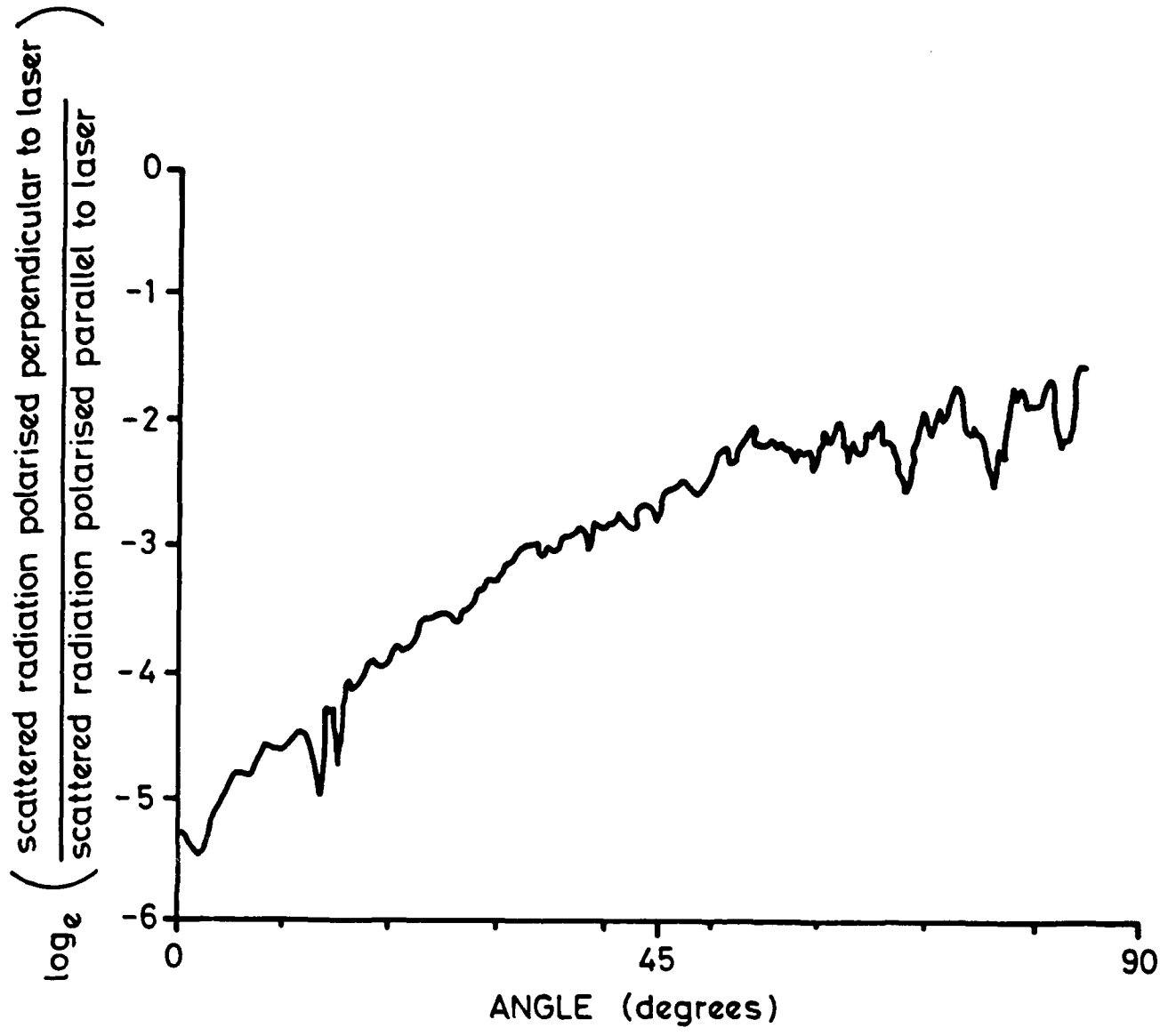

Figure 8 Angular distribution of ratio of cross-polarised to polarised components of CO_2 radiation scattered from the germanium target

REPORT DOCUMENTATION PAGE

DRIC Reference Number (If known) .....

Overall security classification of sheet .....Unclassified.....

(As far as possible this sheet should contain only unclassified information. If it is necessary to enter classified information, the field concerned must be marked to indicate the classification eg (R), (C) or (S).

Originators Reference/Report No.	Month	Year
MEMO 4348	MARCH	1990

Originators Name and Location
RSRE, St Andrews Road
Malvern, Worcs WR14 3PS

Monitoring Agency Name and Location

Title
THEORETICAL AND EXPERIMENTAL COMPARISON OF INFRA-RED AND VISIBLE LASER SCATTERING FROM A VARIETY OF SURFACE TYPES

Report Security Classification	Title Classification (U, R, C or S)
Unclassified	U

Foreign Language Title (in the case of translations)

Conference Details

Agency Reference	Contract Number and Period

Project Number	Other References

Authors	Pagination and Ref
JORDAN, D L; HOLLINS, R C; JAKEMAN, E; PREWETT, A	20

Abstract

A comparison is made between theoretical predictions of the angular distribution of laser radiation scattered from a variety of rough surfaces and experimental measurements of fractal one. The surfaces were initially well characterised using a mechanical stylus instrument to determine the surface profiles. Scattering experiments were then carried out using both transmissive and reflective geometries and both visible and infra-red radiation. The results show that fractal models are appropriate in the infra-red region, whereas single scale models give better agreement with experimental results in the visible region.

Abstract Classification (U,R,C or S)
U

Descriptors

Distribution Statement (Enter any limitations on the distribution of the document)

Unlimited